ACS OMEGA

http://pubs.acs.org/journal/acsodf

Review

Tools of the Trade: Image Analysis Programs for Confocal Laser-Scanning Microscopy Studies of Biofilms and Considerations for Their Use by Experimental Researchers

Shreeya Mhade and Karishma S Kaushik*

Cite This: *ACS Omega* 2023, 8, 20163−20177

Read Online

ACCESS | Metrics & More | Article Recommendations

ABSTRACT: Confocal laser-scanning microscopy (CLSM) is the bedrock of the microscopic visualization of biofilms. Previous applications of CLSM in biofilm studies have largely focused on observations of bacterial or fungal elements of biofilms, often seen as aggregates or mats of cells. However, the field of biofilm research is moving beyond qualitative observations alone, toward the quantitative analysis of the structural and functional features of biofilms, across clinical, environmental, and laboratory conditions. In recent times, several image analysis programs have been developed to extract and quantify biofilm properties from confocal micrographs. These tools not only vary in their scope and relevance to the specific biofilm features under study but also with respect to the user interface, compatibility with operating systems, and raw image requirements. Understanding these considerations is important when selecting tools for quantitative biofilm analysis, including at the initial experimental stages of image acquisition. In this review, we provide an overview of image analysis programs for confocal micrographs of biofilms, with a focus on tool selection and image acquisition parameters that are relevant for experimental researchers to ensure reliability and compatibility with downstream image processing.

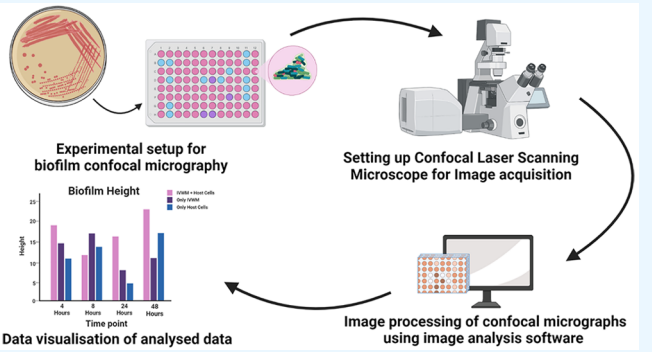

INTRODUCTION

Biofilms are aggregates or clumps of microbial cells, most often bacteria and fungi, attached to a surface or each other and embedded in a self-produced extracellular matrix.[1] Since their first description in 1978,[2,3] biofilms have been increasingly observed across a range of healthcare and environmental settings. Clinical biofilm infections include pneumonia (particularly in diseased lungs), eye, ear, skin, and wound infections, as well as life-threatening cardiac and endovascular infections,[4−6] and are notoriously tolerant to antibiotic treatments. In the environment, biofilms play a role in bioremediation, biofiltration and wastewater management but are also associated with biofouling and food contamination.[7,8] These clinical and environmental implications have prompted the study of biofilms under native and laboratory conditions, using an array of technologies across molecular and microbial scales.[9−11] Notably, a large segment of biofilm research includes microscopic visualization,[12−14] which allows direct observations of biofilm formation and development, structure and organization, as well as viability and metabolic activity in the presence of therapeutic agents.[15−18]

CONFOCAL LASER-SCANNING MICROSCOPY FOR BIOFILM STUDIES

Confocal laser-scanning microscopy (CLSM) has emerged as the most widely used imaging technology for the microscopic visualization of biofilms.[11,13,19,20] A versatile and powerful technique, CLSM allows *in situ*, real-time, and nondestructive examination of living biofilms, along with 3D reconstruction of the entire sample.[21] For this, CLSM excites fluorescence signals from different planes within the sample, resulting in multiple image acquisitions from across the depth of the biofilm. CLSM has made possible qualitative observations of clinical, environmental, and laboratory biofilms, which has led to fundamental insights into the formation, development, morphology, structure, and architecture of biofilms under different conditions.[11,17,18,22−27] Further, with certain modifications, CLSM has also been used to assess the viability and

Received: November 11, 2022
Accepted: May 11, 2023
Published: May 26, 2023

Table 1. Overview of Image Analysis Programs for Biofilm Confocal Micrographs with a Focus on Tool Scope and Selection of Relevance to Experimental Researchers[a]

name of the image analysis program	availability for download	operating system requirements	system requirements	user interface	scope of the tool	capabilities	limitations
Bacterial Cell Morphometry 3D (BCM3D)[46]	open-access; available at https://github.com/GahlmannLab/BCM3D.git	Windows 10	requires MATLAB, Jupyter Notebook scripts for training data, Cell Modeller and NiftyNet	MATLAB and Python scripts based	segmentation	ability to study single bacterial cells in biofilm aggregates; uses deep CNNs with mathematical image analysis to accurately segment and classify single bacterial cells, including in mixed cell populations, from 3D fluorescent images	cannot process images with a low signal-to-background ratio such as images in which objects do not have well-defined structure or edges or high fluorescence; requires understanding of programming languages such as Python and MATLAB for running scripts; requires a MATLAB license, which is expensive
Biofilm Viability Checker[28]	open-access, Macros script available at https://github.com/sophie-mountcastle/Biofilm-Viability-Checker/	Windows, Linux, and macOS	requires MorphoLibJ to run the algorithm, works on FIJI as a plugin	uses the ImageJ interface; the algorithm is a macros script that is run as a FIJI plugin	segmentation; biomass calculation	can process multiple images in a folder at once; low computational time; calculates biomass as percentage coverage of live and dead bacteria in each single-species (live/dead stained) biofilm image	runs only on TIFF files; can only process fluorescent images of single-species biofilms stained with FilmTracer LIVE/DEAD Biofilm Viability Kit; requires understanding of Macros script editing to modify the code to fit the study data
BIAM (Biofilm Intensity and Architecture Measurement)[47,48]	open-access, JAVA based Macros script available at https://github.com/BCinquin/Biofilm_Analysis	Windows, Linux, and macOS	requires 4 GB RAM and ImageJ version 1.51k or later and Java7 to run the script	GUI	segmentation; fluorescence intensity calculation; architectural/structural measurements such as area and perimeter of biofilm	provides intensity calculations for genetic reporters and fluorophores in biofilm; allows intensity correction; uses three different segmentation strategies	TIF files only; can only segment images with a single-labeled fluorophore, not suitable for colocalization studies with two different fluorophores
BiofilmQ[32]	open-access, available for download at https://drescherlab.org/data/biofilmQ/	Windows 10, macOS X, Linux	minimal requirement is Intel i5 with 16GB RAM; requires MATLAB R2017b or subsequent versions	GUI	segmentation using cube cytometry; can measure fluorescence, architectural, and spatial properties; data visualization	accepts input files in 8 different file formats; allows import of presegmented images; provides spatial measurements in images where single-cell resolution is not possible	tool does not work on computers with lower specifications (lower version of processor or less RAM space); when there is heterogeneity in cell sizes, cube segmentation does not work well; tool requires a MATLAB license to run advanced functionality; for batch processing of multiple files, tool requires MATLAB script
BioFilmAnalyzer[49]	free, open-access, and available at https://bitbucket.org/rogex/biofilmanalyzer/downloads/	Windows	no specific requirements mentioned	GUI	segmentation; enumeration of cells; data visualization	counts live and dead cells (can be used for viability counts); can be used for eukaryotic cells (example, host cells in clinical biofilms); quantification of fluorescently labeled subpopulations from 2D micrographs	not available for other OS; Only provides cell count and not structural attributes of cells or aggregates
CMEIAS v3.1[50,51]	free, open-access collection of plugins formerly available at http://cme.msu.edu/cmeias	Windows	requires the UTHSCSA ImageTool for running plugins	GUI of UTHSCSA ImageTool	segmentation; can analyze organizational and structural properties of microbial cells	can categorize microbial cells into 11 predominant bacterial morphotype classes: cocci, spiral, curved rod, U-shaped rod, regular rod, unbranched filament, ellipsoid, club, prosthecate, rudimentary branched rod and branched filaments	runs only on the UTHSCSA ImageTool
CMEIAS Color Segmentation[52]	free, open-access, formerly available at http://cme.msu.edu/cmeias	Windows	run as a module under CMEIAS, requires ImageTools to run CMEIAS	GUI	segmentation	can accurately define biomass object pixels	uses TIFF format only
CMEIAS JFrad[53]	free, open-access, formerly available at http://cme.msu.edu/cmeias	Windows, Linux, and macOS	requires JAVA 6 or higher to run the tool	GUI	measures spatial and architectural biofilm properties such as height,	built to support multiple file formats; user-defined thresholding; allows batch processing	user-defined thresholding can introduce bias

https://doi.org/10.1021/acsomega.2c07255
ACS Omega 2023, 8, 20163−20177

Table 1. continued

name of the image analysis program	availability for download	operating system requirements	system requirements	user interface	scope of the tool	capabilities	limitations
					width, area, and percentage surface coverage using fractal geometry		
COMSTAT[34]	free, open-access, available at www.comstat.dk	Windows, macOS, Linux	requires MATLAB to run the script	command line-based interface	segmentation; biofilm features such as biovolume, area, thickness distribution, mean thickness, identification of microcolonies, and area of microcolonies	user-defined thresholding; quantification of structural elements	requires a MATLAB license, which is expensive; command line-based interface; can only process image formats compatible with MATLAB
COMSTAT2[54]	free, open-access, available at www.comstat.dk	Windows, macOS, Linux	runs as a plugin on ImageJ/FIJI	GUI based on ImageJ-plugin API	segmentation; calculation of structural properties	does not require MATLAB; properties calculated are similar to COMSTAT; can read multiple image formats; multiple thresholding methods	unable to calculate surface-to-volume ratio like COMSTAT
daime[35]	free, open-access available at https://www.microbial-ecology.net/daime	Windows, Linux	requires 1 GB RAM and at least a 512 MB graphic card	GUI	segmentation; capable of noise reduction, filtration, upscaling and downscaling of resolution; data visualization	no programming skills needed; can also analyze conventional epifluorescence, bright field, or phase contrast micrographs; special tools for biofilm image analysis; allows quantification of fluorescence intensity, population abundance, spatial arrangements, morphometry, and object classification; visualization using interactive volume rendering, ray tracing, and 3D image clipping; special image analysis function for identifying correct stringency of new rRNA-targeted probes for FISH; connectivity with R	input images should be in TIFF format only
ISA3D[55,56]	free, open-access	no specific details mentioned	no specific details mentioned	MATLAB based script	segmentation; calculation of structural parameters	offers automated thresholding; can calculate textural and volumetric parameters of biofilms	no download link available
Iris[57]	free, open-access, available at http://critichu.github.io/Iris	Windows, Linux, macOS	requires ImageJ-based API or plugin to run the tool	GUI	segmentation; calculates colony morphology and kinetics data, phenotypic and genotypic activity	ImageJ based so does not require additional software installation; high-throughput and works well for colony arrays; can quantify kinetics data for time series experiments	quantification of kinetics data requires R; programming packages to plot growth curves; requires colony array to be in grid format
PHLIP[58]	free, open-access, available at https://sourceforge.net/projects/phlip/	Windows, Linux, macOS	MATLAB toolbox-based script	GUI	segmentation; biofilm volume, morphology, and surface characterization	allows batch processing; offers both manual and automated (Otsu's Method) thresholding; multichannel analysis; biofilm spatial and temporal calculations: biovolume, substratum coverage, thickness, roughness and colocalization; offers a data conversion option (PHLIP-ML) to convert different image formats to input format; has direct connectivity to PHLIP-ML (file convertor) for Leica Systems	MATLAB-based and requires MATLAB licensing; requires preprocessing steps such as image inversion and x-section resolution
qBA algorithm[59]	free, open-access, available at https://www.infectognostics.de/forschung/technologien/qba-algorithm	Windows, Linux	no specific details mentioned	MATLAB based script	segmentation; bacterial count enumeration	viability counts	designed for counting bacterial cells; based on an adaptive algorithm (rather than binary segmentation); no GUI; requires MATLAB and understanding of MATLAB scripts for troubleshooting
R based method for biofilm thickness by Frühauf et al.[60]	free, open-access R script	Windows, Linux, macOS	R software packages, data.table, reshape2, dplyr, ggplot2, and cowplot	R program GUI)	biofilm thickness calculation	calculates biofilm thickness using a statistical program	only processes UTF-8 encoded import data; requires histogram data of fluorescence intensity for each ROI imported from LAS X software; no automated image segmentation; can calculate only one parameter (biofilm thickness)

https://doi.org/10.1021/acsomega.2c07255
ACS Omega 2023, 8, 20163−20177

Table 1. continued

name of the image analysis program	availability for download	operating system requirements	system requirements	user interface	scope of the tool	capabilities	limitations
ImageJ for biofilm analysis[61,62]	free, open-access, available at https://imagej.nih.gov/ij	Windows, Linux, and macOS	requires JAVA	GUI	segmentation; calculates structural and spatial attributes such as aggregate size, biomass distribution, biomass thickness, biomass intensity, to name a few	processes multiple image formats; generate histograms and profile plots; allows creation of customized Macros script for sharing protocols; connectivity with many microscope customized softwares, e.g., LAS X	requires plug-ins to be separately installed; it is a general image analysis tool and does not offer advanced parameter calculations or options specific for biofilms
ParaView[63]	free, open-access, available at https://www.paraview.org/	Windows, Linux, and macOS	requires visualization toolkit	GUI	data visualization and rendering	allows batch-processing; generates high-quality 3D rendering	requires .vtk files; offers only visualization
Napari[64]	free, open-access, available at https://napari.org/	Windows, Linux, and macOS	requires Python 3.7 or higher; requires Python libraries and packages, Qt library for graphic user interface, VisPy for rendering	Python -based script and GUI	data visualization and rendering	allows creation of customized plugins; generates high-quality 3D rendering	offers only visualization; requires understanding of Python for troubleshooting
Three-Dimensional Biofilm Image Reconstruction Algorithm[19]	no details available	Linux	requires MATLAB R2016a	MATLAB based script	image reconstruction	3D image reconstruction for calculation of structural parameters	requires MATLAB; runs only on Linux; no GUI
Python based method for measuring bacterial biofilm morphology and growth calculation by Gingichashvili et al.[65]	Free, open-access, available at https://github.com/cohenoa/An-Open-Source-Computational-Tool-for-Measuring-Bacterial-Biofilm-Morphology-and-Growth-Kinetics	Windows	requires Python 3 or higher; requires Python libraries and packages	Python based script	segmentation; morphology and growth calculations	macrocolony calculation; fluorescence intensity calculations; can calculate growth kinetics and distance of macrocolony to antimicrobial source	only Otsu's thresholding method can be used; morphological calculations done at the core of the colony

[a]Abbreviations: CNN, convolutional neural network; GUI, graphic user interface; CMEIAS, Center for Microbial Ecology Image Analysis System; daime, digital image analysis in microbial ecology; ISA3D, Image Structure Analyzer in 3D; PHLIP, phobia laser scanning microscopy imaging processor); qBA, quantitative biofilm analysis and bacteria generator.

https://doi.org/10.1021/acsomega.2c07255
ACS Omega 2023, 8, 20163−20177

species diversity within biofilms.[22,28] More recently, the application of CLSM for biofilm studies is moving beyond descriptive observations alone, toward a more in-depth characterization of biofilms from high-resolution image stacks.[17,29,30] For this, CLSM is combined with image analysis tools, which can together provide quantitative insights into biofilm features under different conditions.[31−33] These image analysis programs include not only broadly applicable image processing tools, such as ImageJ and IMARIS, but also programs that are tailor-made to the study of biofilms, such as COMSTAT,[34] daime,[35] and BiofilmQ,[32] to name a few. This shift in the field is reflected across several previous reviews, which focus on microscopy applications and approaches, and image analysis tools and techniques for various biofilm components, including single cells or small groups of bacterial cells, across different scales.[17,33,36−45] In this review, we present an account of the considerations related to confocal micrograph acquisition and processing for biofilm experimental research and provide an in-depth overview of image analysis programs for biofilm confocal micrographs, including their scope, user requirements, and limitations. While the present suite of programs provides the biofilm researcher with an array of options, the specifications for each tool, including their scope, suitability, and limitations, require significant consideration (Table 1). Further, given that biofilm experiments are time-, resource-, and labor-intensive, this overview will be particularly important for biofilm researchers to ensure reliability and compatibility between the experimental setup and downstream image analysis.

GENERAL CONSIDERATIONS FOR CONFOCAL MICROGRAPH ACQUISITION AND PROCESSING FOR BIOFILM STUDIES

The process of extraction of quantitative properties of biofilms from confocal micrographs is a multistep process, starting with the experimental setup and initial acquisition of the micrographs, followed by the subsequent export of images and visualization and analysis of confocal micrographs. While computational image analysis tools enable automated analysis of confocal biofilm micrographs, a basic understanding of the image acquisition process and parameters is important to ensure that the experimental setup is compatible with the subsequent image analysis.

Basics of Confocal Micrographs of Biofilms. Confocal laser scanning microscopy is based on the selective collection of point-by-point fluorescence signals from optical sections within the sample.[66] For confocal biofilm microscopy, bacterial or fungal cells are typically tagged with fluorophores or stained with fluorescent stains or probes.[30,67−69] Following the photon excitation of fluorophores using a laser (gas lasers such as argon-ion, helium−neon, dye lasers, solid-state lasers,[70] and mercury and xenon arc lamps[71]), the detected electrical signal is converted to gray scale values, which correspond to pixel intensity in that region (grayscale intensity values lie between 0 and 255, where 0 means black, 255 means white, and numbers in between represent shades of gray ranging from black to white). Done at high speed by a digitizer at the back-end of the software, this enables real-time visualization and microphotography of the sample. CLSM micrographs are 2D arrays or matrices, consisting of a fixed number of elements or "pixels", each with a particular location (x and y coordinates, in the plane of the sample) and a fixed intensity value.[72−76] The image information is temporarily stored in the computer and displayed on the monitor enabling real-time visualization and microphotography of the sample.[77] The micrographs are typically acquired as a series of optical sections (Z-stacks or Z-layers, that are perpendicular to the optical axis), which are stacked together and reconstructed to produce a 3D representation of the sample.[78] For this, the object within the sample is built up pixel-by-pixel from the detected signal, with each pixel having four horizontal and vertical neighbors. The entire sample is displayed using mathematical operations on the array, where two pixels with the same dimensions (either with coordinates that match or intensities that are the same) are paired together, leading to the final 3D image construction.

Experimental Setup for Biofilm Confocal Micrography. CLSM has been used for acquiring biofilm micrographs from a range of experimental setups such as microtiter wells, colonies on agar, flow cells, microfluidic devices,[22,65,79−81] as well as large volume receptacles.[82] Irrespective of the setup, biofilm experiments tend to show significant variability, even under nearly identical conditions.[83,84] To account for this, it is recommended that biofilm experiments are performed in at least three biological replicates, where each biological replicate is set up from a separate overnight bacterial or fungal culture.[85] Further, for each biofilm replicate, images should be acquired from multiple fields of view, data from which can then be consolidated for a single data point for that replicate. For time-series studies, to account for the effect of prolonged laser exposure on the bacterial or fungal cells, the experiment may need to be set up with multiple technical replicates (the same biofilm set up in different wells), each imaged at a different time point.[30] This setup will allow a technical replicate to be exposed to the laser only for one time point, thereby precluding the effects of photobleaching or phototoxicity of the biofilm sample across multiple time points. In addition, for comparisons across conditions such as different treatments or time points, it would be important to ensure identical parameters of laser intensity, object magnification, and image resolution, as far as possible. Finally, there are guidelines to address variability and ensure repeatability and reproducibility in the setup of biofilm experiments, including standards for reporting minimum information about a biofilm experiment (MIABie) and the design of biofilm imaging experiments.[83,86,87]

Image Acquisition. With currently available commercial CLSM systems, there are only a few critical parameters that need manual adjustments. While researchers are typically familiar with adjustments related to object magnification and optical section thickness, prior acquaintance with additional relevant CLSM settings can significantly improve micrograph quality and reliability.

Scan Speed and Pixel Dwell Time. An important initial consideration during CLSM imaging is scan speed or data acquisition time.[88−91] Scan speed depends on the type of CLSM system used, as well as the optical magnification, numerical aperture, and lateral and axial resolution. Pixel dwell time is the amount of time that a laser beam is allowed to rest on a single pixel in the image.[92] Typically, dwell times of 6−12 μs are sufficient to get reasonable image parameters.[93] Higher resolution images typically require more dwell time per pixel to collect more photons per pixel and therefore a slow scan speed. However, setting a higher value for dwell time can increase the risk of photobleaching of the specimen.[91] There is therefore a trade-off between achieving high spatial and temporal

https://doi.org/10.1021/acsomega.2c07255
ACS Omega 2023, 8, 20163−20177

resolution and scan speed, given that longer scanning and acquisition times could result in photodamage.[94]

Laser Intensity. Given that CLSM micrograph acquisition is based on the intensity of fluorescent signals, the selection of the type and power of the laser are important considerations at the start of the image acquisition process. Typically, the selection of the laser and wavelength depends on the excitation and emission spectra of the fluorophores in the experimental setup.[95−97] For this, it is important to understand the spectral and physical properties of fluorophores or fluorescent stains or probes; Fluorescence SpectraViewer[98] is an interactive tool that can be used to select probes and filters for fluorescence-based experimental design. Finally, while setting the laser intensity can vary across samples and experimental conditions, it is important to consider the effects of laser intensity on the micrographs. At low laser intensities, valuable signal information from the micrographs may be missed, whereas higher laser intensities can lead to signal saturation and photodamage. Notably, several acquisition software programs display autohistograms, which can help with laser intensity adjustments.[88,91,99] Finally, for time-series experiments, the laser intensity may have to be adjusted across time points. This is relevant in the context of biofilm growth over time, where bacteria grow to form large mats of biomass, in which case the fluorescence intensity of the sample is likely to increase, or with the effect of treatments, in which case the intensity could decrease. In this case, adjustments to the laser intensity might be needed, and this should be considered when performing and interpreting downstream image analysis. For example, when analyzing and comparing intensity values, biofilm time points or conditions exposed to different laser intensities would need to be normalized to ensure accurate interpretation of the values.

Pinhole Diameter. In CLSM systems, a portion of the emitted fluorescence is collected by the objective lens and focused into a pinhole in front of the detector.[100] The amount of fluorescent light that reaches the detector is determined by the detector pinhole. While the diameter of the pinhole is usually set at ∼1 Airy unit, it is important to note that the pinhole aperture determines the thickness of the optical section and can therefore influence the resolution of the micrographs.[88,91,99] A larger pinhole diameter will result in more extrafocal intensity reaching the detector and could compromise the sharpness of the optical sections. However, for low fluorescence signals or fading fluorescence, the user may need to open the pinhole to capture as much fluorescence as possible, which can compromise the *Z*-resolution of the micrographs.[101] For multicolor or multichannel images, for a consistent optical slice or *Z*-layer resolution, it is crucial that the pinhole size is adjusted depending on the wavelength of the emitted light.[102−104]

Penetration Depth. Confocal laser scanning microscopy is primarily based on capturing a portion of the nonscattered emitted fluorescence that originates at the focal plane of the objective lens.[77] Absorption and scattering of laser light cause a significant reduction in image quality in thicker biofilm samples, as the intensity of fluorescence in different sections of the biofilm sample can differ due to laser attenuation. The laser intensity in the lower section decreases as the penetration depth increases because a significant fraction of the excitation light is absorbed in the top layers of the sample, resulting in less excitation light reaching the deeper layer of the biofilms. This laser attenuation property, a critical aspect during confocal microscopy image acquisition, is well predicted and governed by the Beer−Lambert Law, which explains how light absorption exponentially decays as the laser is focused deeper into a specimen.[105−108] This results in artificially low fluorescence intensities in the biofilm's deeper layers, which is caused by spherical aberration of the objective lens.[77,109,110] Because the configuration of confocal microscopy systems is based on using the same optical lens for fluorescence excitation and detection,[77,100] the excited beam passing through the outermost edge of the lens focuses at a different point on the axial plane than the beam passing through the center of the lens. The emitted light suffers from the same spherical aberration, which significantly reduces image resolution.[105] As a result, it is critical to consider that image resolution is compromised at depths greater than 50−80 μm.[105,108] To overcome this challenge to some extent, advanced confocal microscopy techniques such as multiphoton confocal microscopy or advanced statistical methods during image analysis could be used.[106,108,111]

Zoom Settings. In general, the zoom control varies the size of the area of the specimen scanned, and typically there is only one optimal zoom setting for a particular combination of wavelength, numerical aperture, and objective magnification. This setting provides a pixel size that matches the Nyquist criterion,[88,112] which states that the pixel size of an image needs to be at least 2.3 times smaller than the object being resolved, and can be calculated with an online Nyquist calculator.[113] Notably, suboptimal zoom settings can result in over-sampling or under-sampling of data.[112] For example, the diffusion of certain dye molecules can cause a small variation in fluorescence intensity, and in this case, choosing a higher spatial resolution could result in a large pixel-to-pixel variation. For confocal micrographs of biofilm mats or aggregates, images of 512 × 512 or 1024 × 1024 pixels with a resolution of 300 dpi are widely used.[59,88,112,114] While spatial resolution corresponds to image quality, setting a higher resolution may increase the image acquisition time and could also lead to photobleaching or photodamage.[87,115]

Z-Thickness and Step Size. An important consideration during CLSM image acquisition is adjustments to the *Z*-thickness of the acquired micrographs.[91,116] Current CLSM systems possess built-in features that enable scanning of the sample across the *Z*-axis in "live" mode.[117] Following this initial scanning, the lower and upper *Z*-layers are typically set to include the lowermost and uppermost regions of the biofilm sample.[30,31] Given that the number of *Z*-slices, and therefore the total *Z*-stack size, may vary across replicates, this may have to be set manually for each experimental replicate or condition. A step size of 1−2 μm is typically used to cover the entire biofilm sample.[31,87,118] While the step size can be increased or decreased, this has to be considered in the context of the experimental setup; decreasing the step size would result in thinner optical sections for more accurate 3D reconstruction, while increasing the step size would result in faster image acquisition.

Taken together, image acquisition parameters for biofilm confocal micrography can be adjusted using commercial acquisition software systems, depending on the type and version of the CLSM system being used.[38,118,119] For Leica SP8 Confocal systems, an online tool is available to calculate the zoom factor and *Z*-step size.[120]

Additional CLSM Features for Image Acquisition. For large specimens (such as entire organs, organisms, or

https://doi.org/10.1021/acsomega.2c07255
ACS Omega 2023, 8, 20163−20177

microtiter wells), the mosaic function in CLSM systems can be used for visualization at high resolution.[121,122] This function combines multiple images into a single, large superimage of the specimen. A tile scan, which records a set number of adjoining single images of the sample (the "tiles"), is required for such a stitched superimage.[66,79,84] While the sample is moved using the motorized stage to ensure precision, a small percentage (2−10%) of overlapping pixels between single images is required to perfectly match the tiles.[123] Certain CLSM systems also allow you to define two reference points (bounding box) at opposite corners of the specimen, and then the number and position of the fields to cover the specimen, including predefined overlapping regions, are calculated. The mosaic function is not limited to *xy* images (2D) but can also be used to generate large 3D images.[39,124,125] Finally, high content screening confocal laser microscopy (HCS-CLM) employs a special mode to improve raw data quality (higher resolution) through the use of predefined and fully customizable automated analysis (unbiased) workflows (faster acquisition).[126] Used to study 4D structural dynamics of biofilms in 96-well microplates, this computer aided microscopy (CAM) tool allows the user to create a scanning template or workflow that is suitable for the experimental conditions. The raw data generated from this tool is usually in a platform-independent OME-TIFF format, which is compatible with several image analysis tools.

Exporting Confocal Micrographs from CLSM Systems. In addition to basic features for image acquisition and analysis, commercial CLSM software systems include several options for exporting and saving confocal micrographs.[91] Along with the image, the software allows additional data to be saved in manufacturer-customized or proprietary image formats, such as the image number, date of acquisition, microscope settings, exposure values, as well as the size and scale details of the image (for example, .lif for Leica systems, .czi for Zeiss microscopes, .nd2 for Nikon, and .oib for Olympus microscopes).[127] Confocal micrographs are typically saved as 8-bit images, with each pixel of the cross-section with intensity values in the gray value range of 0−255, though higher bit depths (12-bits) can also be generated with intensity values in the gray value range of 0−4095.[90] However, higher bit depths necessitate more file memory space, and certain image analysis software programs cannot read 12-bit images. Several CLSM softwares also provide the option of batch-exporting and batch-processing of several exported images at once; a notable example is the Batch Tools Workspace in the ZEN Blue software (Zeiss).[117,128] While CLSM systems allow users to save images in various formats, it is recommended that users use the manufacturer's image format. These customized image formats can then be converted into universal and platform-independent formats such as .tiff, ome-tiff, .jpeg, or .png using the BioFormats plugin (available in ImageJ[61] and FIJI[129]). It is important to note, however, that recently developed image analysis tools obviate the need for a separate conversion to .tiff (by incorporating a BioFormats plugin into their source code), and several customized image formats, such as Nikon NIS-Elements ND2 files (.nd2), Zeuss CZI files (.czi), Zeiss LSM (laser scanning microscope) 510/710 files (.lsm), Leica LAS AF LIF (Leica Image File Format) files (.lif), and Olympus FluoView FV1000 files (.oif or .oib), can be directly imported in formats compatible with image analysis programs.[97] A notable example is the image analysis program BiofilmQ, with file input and recognition features for standard microscope file types and conversion of these files into an internal format.[32]

Image Processing of Confocal Micrographs. Following the export of confocal micrographs from the CLSM system, the imported images need to undergo initial processing for object identification and analysis.[33,130] The general image analysis pipeline for biofilm studies is divided into three sections: image preprocessing, image segmentation, and feature extraction and analysis. Image preprocessing techniques such as median filtering, background subtraction noise reduction, signal attenuation correction, sharpness, edge detection, and the deconvolution algorithm can aid in the reduction or removal of unwanted image artifacts. It is important to note, however, that these preprocessing steps can be computationally expensive, and caution should be exercised when fine-tuning the preprocessing parameters to ensure that unwanted artifacts are removed without losing the object of interest.[131] Before one can extract morphological and functional measurements from a micrograph, it is important that there is discrete identification or labeling of voxels. Each pixel (or voxel, volumetric pixels in 3D micrographs) in a confocal micrograph has a distinct gray value that corresponds to the intensity of the captured signal.

Image segmentation[130−133] refers to the process of transitioning voxels from a conceptually simple array of point measurements of fluorescence intensity to the more informative concept of image objects. Regions and boundaries are two commonly used concepts in image segmentation. Techniques for image segmentation can be divided into three categories: bottom-up methods, top-down methods, and hybrid methods.[131] Bottom-up methods rely on identifying regions that represent objects of interest and iteratively merging voxels with similar measures. The top-down approach requires some prior knowledge about object shapes, object models, and the number of regions; however, this requirement for some level of knowledge tends to limit the applicability of this segmentation approach. Finally, the hybrid method combines both the bottom-up and top-down approaches and can be computationally demanding.

The bottom-up method can be further divided into four categories: intensity thresholding, region-based, boundary-based, and integrated segmentation. In the intensity-based thresholding approach, a threshold is applied and all voxels whose values lie within a certain range of fluorescence intensity belong to one class. This is done to separate the object of interest (in case of biofilms, biomass) from the background. This results in image binarization (1 for biomass and 0 for background).[82,134] A voxel is considered a background voxel if its shade intensity is less than the threshold value, else it is considered a biomass voxel.[133,135] Each voxel in the segmented image contains information about the object class to which it belongs, with background voxels having a zero-voxel value. Using a single threshold value for an entire image allows for global thresholding of the image. Adaptive or local thresholding occurs when the threshold value changes for different regions of the image. Local thresholding is applied under specific conditions such as when the user needs to select an individual threshold for each pixel. For local thresholding, the image needs to be cropped into small sections and each section is thresholded using the selected method.[72,136] The region-based segmentation method assumes that neighboring voxels within a specific region of an object are homogeneous. The general procedure in region-based segmentation is to compare

https://doi.org/10.1021/acsomega.2c07255
ACS Omega 2023, 8, 20163−20177

each voxel to its neighbors. If the homogeneity criteria are met, the voxel is said to belong to the same class. However, the performance of this approach is heavily reliant on the choice of homogeneity criteria. The boundary-based approach, on the other hand, is heavily reliant on edge detection and the integration of boundary information for classification. These edges identify image discontinuities in gray levels, color, texture, and so on, and aid in image segmentation. Lastly, integrated segmentation combines the characteristics of both region and boundary criteria; a notable example is the watershed algorithm,[137] which is based on an integrated segmentation approach. In recent years, there has been an increase in the development of novel segmentation approaches based on convolutional neural networks and deep learning, with DeepCell 2.0[138] and CellProfiler 3.0[139] being notable examples. However, CLSM biofilm image segmentation typically employs a traditional thresholding technique that selects a threshold value to segment voxels in the images based on fluorescence or grayscale intensity.

Thresholding in biofilm studies can be performed either manually or automatically and can be applied to individual 2D images or applied together for a stack of confocal micrographs. Manual thresholding relies on the visual determination of thresholds[140] and is therefore prone to bias in the measurement of biofilm features, where setting a low threshold can falsely capture the presence of biomass when there is none and a threshold that is too high can result in missing the measurements of low-intensity biomass.[31,55,82,130] Automated thresholding methods can be global or local, depending on the specificity and sensitivity needed for the detection of the regions of interest. Otsu's thresholding approach, which is used in software such as COMSTAT and BiofilmQ, is a widely used global method based on traditional segmentation that selects an optimum threshold that can provide maximum variation in shade intensity and class separability between the biomass and background.[141] Other global methods include iterative selection[142] in software like BiofilmQ and daime, robust automatic threshold selection (RATS)[143] in software like daime, and objective threshold selection (OTS)[144] in software like PHLIP. Notably, several recently available tools for biofilm analysis are based on Otsu thresholding and iterative selection.[31,55]

Under certain experimental conditions, it could be difficult to distinguish individual microbial cells in the image, for example, in confocal micrographs of dense biofilm aggregates or mats. In this case, the pixel location of the biofilm edge may not be uniquely defined, given that the biofilm edge consists of a fluorescence signal gradient that can span several cell diameters.[31,55] As a result, different segmentation algorithms will identify the biofilm edge in slightly different locations. Because images of microbial communities without single-cell resolution are frequently analyzed in biofilm research, the need for accurate semantic segmentation has resulted in a range of different algorithmic solutions for biofilm analysis such as Bacterial Cell Morphometry 3D (BCM3D),[46] BiofilmQ,[32] daime,[35] and qBA algorithm.[59]

SPECIFIC EXPERIMENTAL CONSIDERATIONS FOR IMAGE ACQUISITION AND ANALYSIS FOR BIOFILM CONFOCAL MICROGRAPHS

The first step in the analysis of biofilm confocal micrographs is the selection of an image analysis program that is best suited to the parameters under study. Because this decision affects all subsequent processing steps, it is beneficial for the experimental researcher to understand the tools available and determine the most suitable tool for the desired analysis. It is important to note that the experimental study may require a combination of several tools to analyze different biofilm features. Recent reviews provide a list of comprehensive points of consideration, which can be used as a starting point for tool selection.[17,33,36−45] In addition, based on our experience, we suggest certain experimental factors which would be valuable to consider at the start of and during the biofilm confocal micrograph acquisition and analysis process.

What Are the Biofilms and Other Biological Elements in the Biofilm Confocal Micrographs Expected to Look Like? Depending on the bacteria and fungi under study, biofilms typically grow from single cells or clumps of cells to larger aggregates and dense mats of biomass.[145−150] Growth conditions, including *in vitro* platforms and media conditions are known to influence biofilm properties.[11,84,151,152] Taken together, a combination of biofilm features, including the spatiotemporal distribution, biomass intensity, and biofilm components (bacterial or fungal cells, matrix) and morphology (single cells, aggregates, dense mats, pellicles), will constitute the raw data set of the confocal micrographs. In the case of clinical and *in vivo* biofilms, host tissue and cellular factors may also be imaged.[153−156] In the case of environmental biofilms, plant structures and additional biological elements (diatoms, algae) may also be present in the sample.[157−160] Identifying and analyzing these biofilm and non-biofilm features may require special consideration at the time of image acquisition (laser intensity, zoom factor, *Z*-slice thickness, presence of autofluorescence) to ensure appropriate image processing and tool selection.

What Are the Analysis Parameters Needed for the Study? At the stage of image acquisition, it would be important to consider the downstream processing and analyses needed for the goals of the experiment. This is relevant not only for tool selection but also for ensuring that the experimental conditions and image acquisition parameters meet these requirements. For example, if biomass thickness is expected to be a parameter under study, it would be optimum to select multiple regions of the biofilm for imaging for each replicate, which can then be pooled to obtain biomass thickness for that replicate. This would account for variability in thickness across different regions of the replicate (for example, in a 96-well).[83,84] Another example would be quantifying biofilm aggregate dimensions, which can be done using area or volume, using growth rate as a proxy measure.[30,161,162] For the size of the aggregates, a *Z*-stack projection would provide details about area and mean gray value for each aggregate cluster, which can be computed using several available programs.[32,34,35,48,53,54,58,59,61] Quantification of aggregate volume would require high-resolution images and user familiarity with advanced tools such as BiofilmQ,[32] COMSTAT,[34] COMSTAT2,[54] Iris,[57] ISA3D,[56] PHLIP,[58] qBA algorithm,[59] with features to quantify the biovolume of each aggregate. Finally, an aggregate can also be quantified using growth rate as a proxy measure, using biomass measurements as a function of time.[162]

In the Case of Time-Lapse and Treatment Experiments, How Is the Image Acquisition and Analysis Likely to Change Across the Experiment? The growth of biofilms over time and the effects of treatments can cause marked shifts in fluorescence intensity from the sample, which

https://doi.org/10.1021/acsomega.2c07255
ACS Omega 2023, 8, 20163−20177

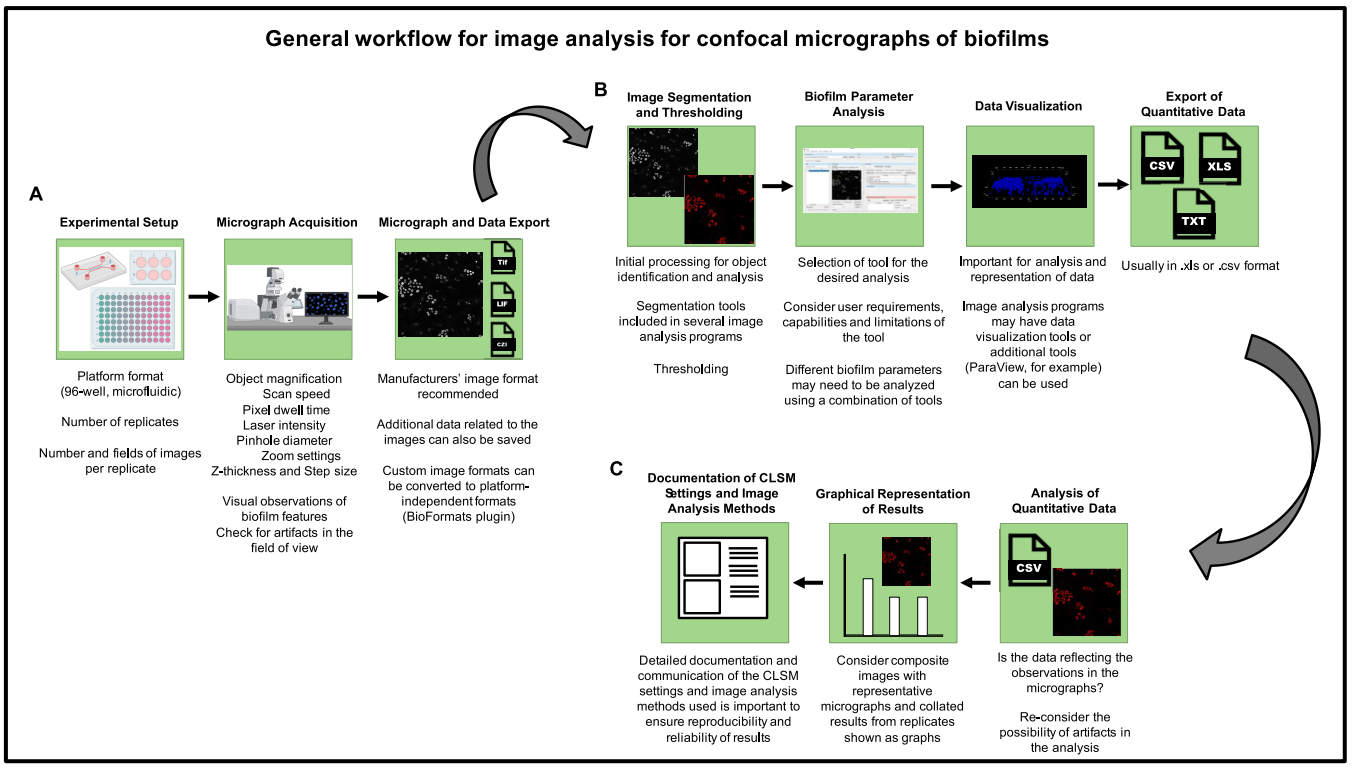

Figure 1. General workflow for analysis of confocal micrographs of biofilms can be divided into (A) experimental setup and image acquisition, (B) image processing, visualization and analysis, and (C) analysis of quantitative data and representation of results. Understanding the confocal micrograph acquisition process and parameters as well as the selection and scope of the image analysis programs is important to ensure compatibility between the experimental setup and subsequent image analysis.

will require modifications in image acquisition settings.[30,163,164] For example, the formation of large, dense biomass mats could increase the fluorescence intensity from the biofilm, prompting a decrease in the laser intensity. On the other hand, reduction in biomass following antibiotic or antimicrobial treatments could require an increase in laser intensity to visualize the remnant biomass.[165] This can also be the case when studying spatial and temporal biofilm features, such as biofilm morphology and viability, which could demonstrate heterogeneity across the experimental time points.[164] Importantly, these changes in settings will need to be accounted for during the image analysis, to prevent erroneous conclusions from the experiments. While the considerations will vary based on experimental conditions, this can be possibly overcome by preliminary determination of a "sweet spot" of CLSM settings that works across time points and conditions. Alternatively, the differences in CLSM settings can be accounted for by normalizing the data or representing the data as ratios across time points. For example, the intensity of the biomass at a subsequent time point can be normalized to the biomass intensity at the initial ("zero" time point[30,166]).

How Does the Experimental Researcher Plan to Represent the Data for a Given Biofilm Feature or Parameter? While the graphical representation of data related to biofilm features and parameters will likely be finalized only after the image processing and analysis, it is worthwhile to consider how the experimental conditions could influence the final representation of data. Given the nature of biofilm experiments, including the substantial variation observed across replicates, data representation is particularly important in the context of spatial studies of biofilms.[30,147,148] For example, when analyzing the spatial organization of biomass in a given condition, the location of the upper and lower bounds of the biofilm can vary across replicates. The biofilm replicates may not be attached all the way to the top or start at the same location at the base of the well or extend across the same height in the well. In this case, representing the data for each replicate separately could be considered.

Are There Possible Artifacts in the Image Acquisition Process That Should Be Considered at the Time of Analysis? During the image acquisition process, it is important to make a visual note of the biofilm features observed and check for possible inconsistencies, which could result in the misrepresentation of results from downstream image analysis.[84] Given that image analysis programs will analyze biofilm features irrespective of whether they are native phenomena or artifacts, it is for the experimental researcher to determine if the observations are real. For example, when measuring biomass distribution, the dispersal of biomass due to technical errors (such as perturbation of the biofilm in a 96-well-plate due to physical movement or pipetting) could erroneously increase the vertical biomass distribution width. This would also influence the size and properties of biofilm aggregates and therefore be an artifact in the analysis. Another example of an artifact that could result during aggregate analysis is the presence of dense aggregates, as can occur during long periods of biofilm growth.[30] In this case, the inability to distinguish between closely placed aggregates might result in larger aggregate dimensions as readouts. Therefore, while a particle size analysis tool (such as ImageJ) will provide a distribution of aggregate dimensions regardless of the biomass density, the experimenter should consider the results

https://doi.org/10.1021/acsomega.2c07255
ACS Omega 2023, 8, 20163−20177

of the analysis in conjunction with the visual biofilm features at the time of image acquisition.

Taken together, once a raw set of images have been acquired and a suitable tool for an image analysis task has been identified, new users could use a series of test images to familiarize themselves with the user interface, tool features and options, and analysis sensitivity and results. Further, experimental researchers can also reach out to tool developers for technical challenges, and several tools also have community forums for troubleshooting.

Finally, it is vital for the experimental biofilm researcher to document in detail the CLSM settings used for image acquisition and image processing tools and analysis parameters employed (in the methods section of a manuscript, for example) to ensure reproducibility and reliability of the experimental results. It is evident that several factors in the CLSM image analysis workflow, including the experimental setup, microscopy settings, image segmentation and thresholding, and image analysis parameters (Figure 1), would be important for subsequent researchers to build upon or adapt the biofilm study conditions.

OVERVIEW OF IMAGE ANALYSIS PROGRAMS FOR ANALYSIS OF BIOFILM CONFOCAL MICROGRAPHS

In this section, we present an overview of the tools available for biofilm confocal micrograph segmentation and postsegmentation quantitative image analysis. In particular, we focus on the aspects of tool selection relevant to experimental researchers such as the user requirements, scope, capabilities, and limitations of the program (Table 1). It is important to note that this review focuses on biofilm image analysis at a community level (aggregates, mats of bacterial or fungal cells) and does not extensively cover single-cell biofilm analysis. Further, we have largely focused on conventional image analysis tools, which are widely used and have well-established protocols and technical support. Together, albeit not all inclusive, this will serve as a primary set of image analysis options for the experimental researcher. In doing so, this review will also provide a basic understanding of the process and considerations related to biofilm confocal micrograph analysis which can be applied to specific user scenarios such as single-cell analysis.[33,46,167,168] Further, as image analysis tools expand to account for heterogeneity and density in biofilms, more recent tools incorporate deep learning and neural network approaches to extract biofilm microscale features.[169] While we have not discussed these tools in detail, they are typically based on prior training of a set of data, after which raw images can be analyzed, and their widespread application will be an important advance in biofilm image analysis.

CONCLUSIONS

With a push toward quantitative analysis of biofilms across a range of native and laboratory conditions, familiarity with the requirements and capabilities of image analysis tools are important for the experimental researcher. Overall, it is important to consider the biofilm features and parameters under evaluation at the start of the design and execution of the experiment which could help ensure compatibility between the experimental setup and the image processing pipeline. In addition, considerations such as Operating System (OS) requirements, familiarity with the user interface (codes or scripts, if any) and purchase of licensed software, are also important. Taken together, the current tools of the trade are well-poised to further quantitative biofilm research and, along with recent advances in single-cell analysis and AI/ML based methods, lend themselves well to a fine-tuned analysis of biofilm features from confocal micrographs.

AUTHOR INFORMATION

Corresponding Author

Karishma S Kaushik − *Department of Biotechnology, Savitribai Phule Pune University, Pune 411007, India;* orcid.org/0000-0001-5131-1798; Email: karishmaskaushik@gmail.com

Author

Shreeya Mhade − *Department of Biotechnology, Savitribai Phule Pune University, Pune 411007, India;* orcid.org/0000-0002-3050-802X

Complete contact information is available at: https://pubs.acs.org/10.1021/acsomega.2c07255

Funding

K.S.K.'s appointment is supported by the Ramalingaswami Reentry Fellowship (BT/HRD/16/2006), Department of Biotechnology, Government of India. This work was supported by the Har Gobind Khorana-Innovative Young Biotechnologist Award (IYBA) to K.S.K (BT/12/IYBA/2019/05).

Notes

The authors declare no competing financial interest.

ACKNOWLEDGMENTS

The authors' thank Radhika Dhekane for helpful discussions on confocal microscopy settings and image acquisition for biofilm experiments.

REFERENCES

(1) Costerton, J. W.; Lewandowski, Z.; Caldwell, D. E.; Korber, D. R.; Lappin-Scott, H. M. MICROBIAL BIOFILMS. *Annu. Rev. Microbiol.* **1995**, *49* (1), 711−745.

(2) Costerton, J. W.; Geesey, G. G.; Cheng, K.-J. How Bacteria Stick. *Sci. Am.* **1978**, *238* (1), 86−95.

(3) Hall-Stoodley, L.; Costerton, J. W.; Stoodley, P. Bacterial Biofilms: From the Natural Environment to Infectious Diseases. *Nat. Rev. Microbiol.* **2004**, *2* (2), 95−108.

(4) Vickery, K. Special Issue: Microbial Biofilms in Healthcare: Formation, Prevention and Treatment. *Materials (Basel).* **2019**, *12* (12), 2001.

(5) Lebeaux, D.; Ghigo, J.-M.; Beloin, C. Biofilm-Related Infections: Bridging the Gap between Clinical Management and Fundamental Aspects of Recalcitrance toward Antibiotics. *Microbiol. Mol. Biol. Rev.* **2014**, *78* (3), 510−543.

(6) Høiby, N.; Bjarnsholt, T.; Moser, C.; Bassi, G. L.; Coenye, T.; Donelli, G.; Hall-Stoodley, L.; Holá, V.; Imbert, C.; Kirketerp-Møller, K.; Lebeaux, D.; Oliver, A.; Ullmann, A. J.; Williams, C.; et al. ESCMID Guideline for the Diagnosis and Treatment of Biofilm Infections 2014. *Clin. Microbiol. Infect.* **2015**, *21* (S1), S1−25.

(7) Lens, P. Biofilms for Environmental Biotechnology in Support of Sustainable Development: A Report. *Virulence* **2011**, *2* (5), 490−489.

(8) Vishwakarma, V. Impact of Environmental Biofilms: Industrial Components and Its Remediation. *J. Basic Microbiol.* **2020**, *60* (3), 198−206.

(9) Franklin, M. J.; Chang, C.; Akiyama, T.; Bothner, B. New Technologies for Studying Biofilms. *Microbiol. Spectr.* **2015**, *3* (4), No. 3.4.27.

(10) Highmore, C. J.; Melaugh, G.; Morris, R. J.; Parker, J.; Direito, S. O. L.; Romero, M.; Soukarieh, F.; Robertson, S. N.; Bamford, N. C. Translational Challenges and Opportunities in Biofilm Science: A BRIEF for the Future. *NPJ biofilms microbiomes* **2022**, *8* (1), 68.
(11) Azeredo, J.; Azevedo, N. F.; Briandet, R.; Cerca, N.; Coenye, T.; Costa, A. R.; Desvaux, M.; Di Bonaventura, G.; Hébraud, M.; Jaglic, Z.; Kačániová, M.; Knøchel, S.; Lourenço, A.; Mergulhão, F.; Meyer, R. L.; Nychas, G.; Simões, M.; Tresse, O.; Sternberg, C. Critical Review on Biofilm Methods. *Crit. Rev. Microbiol.* **2017**, *43* (3), 313−351.
(12) Relucenti, M.; Familiari, G.; Donfrancesco, O.; Taurino, M.; Li, X.; Chen, R.; Artini, M.; Papa, R.; Selan, L. Microscopy Methods for Biofilm Imaging: Focus on SEM and VP-SEM Pros and Cons. *Biology (Basel).* **2021**, *10* (1), 51.
(13) Palmer, R. J.; Sternberg, C. Modern Microscopy in Biofilm Research: Confocal Microscopy and Other Approaches. *Curr. Opin. Biotechnol.* **1999**, *10* (3), 263−268.
(14) Alhede, M.; Qvortrup, K.; Liebrechts, R.; Høiby, N.; Givskov, M.; Bjarnsholt, T. Combination of Microscopic Techniques Reveals a Comprehensive Visual Impression of Biofilm Structure and Composition. *FEMS Immunol. Med. Microbiol.* **2012**, *65* (2), 335−342.
(15) Sauer, K.; Stoodley, P.; Goeres, D. M.; Hall-Stoodley, L.; Burmølle, M.; Stewart, P. S.; Bjarnsholt, T. The Biofilm Life Cycle: Expanding the Conceptual Model of Biofilm Formation. *Nat. Rev. Microbiol.* **2022**, *20* (10), 608−620.
(16) Gomes, L. C.; Mergulhão, F. J. SEM Analysis of Surface Impact on Biofilm Antibiotic Treatment. *Scanning* **2017**, *2017*, No. 2960194.
(17) Reichhardt, C.; Parsek, M. R. Confocal Laser Scanning Microscopy for Analysis of Pseudomonas Aeruginosa Biofilm Architecture and Matrix Localization. *Front. Microbiol.* **2019**, *10*, 677.
(18) Huang, Y.; Chakraborty, S.; Liang, H. Methods to Probe the Formation of Biofilms: Applications in Foods and Related Surfaces. *Anal. Methods* **2020**, *12* (4), 416−432.
(19) Ben-Sahil, A.; Mohamed, A.; Beyenal, H. Three-dimensional Biofilm Image Reconstruction for Assessing Structural Parameters. *Biotechnol. Bioeng.* **2020**, *117* (8), 2460−2468.
(20) Lawrence, J. R.; Neu, T. R. [9] Confocal Laser Scanning Microscopy for Analysis of Microbial Biofilms. In *Methods in Enzymology*; Doyle, R., Ed.; Elsevier, 1999; Vol. *310*, pp 131−144. DOI: 10.1016/S0076-6879(99)10011-9.
(21) Lawrence, J. R.; Korber, D. R.; Hoyle, B. D.; Costerton, J. W.; Caldwell, D. E. Optical Sectioning of Microbial Biofilms. *J. Bacteriol.* **1991**, *173* (20), 6558−6567.
(22) Bridier, A.; Dubois-Brissonnet, F.; Boubetra, A.; Thomas, V.; Briandet, R. The Biofilm Architecture of Sixty Opportunistic Pathogens Deciphered Using a High Throughput CLSM Method. *J. Microbiol. Methods* **2010**, *82* (1), 64−70.
(23) Flemming, H.-C.; Szewzyk, U.; Griebe, T. Confocal Laser Scanning Microscopy (CLSM) of Biofilms. *Biofilms: Investigative Methods and Applications*; CRC Press: Boca Raton, 2000; DOI: 10.1201/9781482293968.
(24) Kleine, D.; Chodorski, J.; Mitra, S.; Schlegel, C.; Huttenlochner, K.; Müller-Renno, C.; Mukherjee, J.; Ziegler, C.; Ulber, R. Monitoring of Biofilms Grown on Differentially Structured Metallic Surfaces Using Confocal Laser Scanning Microscopy. *Eng. Life Sci.* **2019**, *19* (7), No. 513.
(25) Neu, T. R.; Lawrence, J. R. Development and Structure of Microbial Biofilms in River Water Studied by Confocal Laser Scanning Microscopy. *FEMS Microbiol. Ecol.* **1997**, *24* (1), 11−25.
(26) Wu, S.; Yang, T.; Luo, Y.; Li, X.; Zhang, X.; Tang, J.; Ma, X.; Wang, Z. Confocal Laser Scanning Microscopy (CLSM) Analysis of Extracellular Polymeric Substances (EPSs) Present in Biofilms. 2014.
(27) Donlan, R. M.; Costerton, J. W. Biofilms: Survival Mechanisms of Clinically Relevant Microorganisms. *Clin. Microbiol. Rev.* **2002**, *15* (2), 167−193.
(28) Mountcastle, S. E.; Vyas, N.; Villapun, V. M.; Cox, S. C.; Jabbari, S.; Sammons, R. L.; Shelton, R. M.; Walmsley, A. D.; Kuehne, S. A. Biofilm Viability Checker: An Open-Source Tool for Automated Biofilm Viability Analysis from Confocal Microscopy Images. *npj Biofilms Microbiomes* **2021**, *7* (1), 44.
(29) Sommerfeld Ross, S.; Tu, M. H.; Falsetta, M. L.; Ketterer, M. R.; Kiedrowski, M. R.; Horswill, A. R.; Apicella, M. A.; Reinhardt, J. M.; Fiegel, J. Quantification of Confocal Images of Biofilms Grown on Irregular Surfaces. *J. Microbiol. Methods* **2014**, *100* (1), 111−120.
(30) Dhekane, R.; Mhade, S.; Kaushik, K. S. Adding a New Dimension: Multi-Level Structure and Organization of Mixed-Species Pseudomonas Aeruginosa and Staphylococcus Aureus Biofilms in a 4-D Wound Microenvironment. *Biofilm* **2022**, *4*, 100087.
(31) Merod, R. T.; Warren, J. E.; McCaslin, H.; Wuertz, S. Toward Automated Analysis of Biofilm Architecture: Bias Caused by Extraneous Confocal Laser Scanning Microscopy Images. *Appl. Environ. Microbiol.* **2007**, *73* (15), 4922−4930.
(32) Hartmann, R.; Jeckel, H.; Jelli, E.; Singh, P. K.; Vaidya, S.; Bayer, M.; Rode, D. K. H.; Vidakovic, L.; Díaz-Pascual, F.; Fong, J. C. N.; Dragoš, A.; Lamprecht, O.; Thöming, J. G.; Netter, N.; Häussler, S.; Nadell, C. D.; Sourjik, V.; Kovács, Á. T.; Yildiz, F. H.; Drescher, K. Quantitative Image Analysis of Microbial Communities with BiofilmQ. *Nat. Microbiol.* **2021**, *6* (2), 151−156.
(33) Jeckel, H.; Drescher, K. Advances and Opportunities in Image Analysis of Bacterial Cells and Communities. *FEMS Microbiol. Rev.* **2021**, *45* (4), fuaa062.
(34) Heydorn, A.; Nielsen, A. T.; Hentzer, M.; Sternberg, C.; Givskov, M.; Ersbøll, B. K.; Molin, S. Quantification of Biofilm Structures by the Novel Computer Program Comstat. *Microbiology* **2000**, *146* (10), 2395−2407.
(35) Daims, H.; Lücker, S.; Wagner, M. Daime, a Novel Image Analysis Program for Microbial Ecology and Biofilm Research. *Environ. Microbiol.* **2006**, *8* (2), 200−213.
(36) Choudhary, D.; Cassaro, C. J. Digging Deeper in the Biofilm. *Nat. Rev. Microbiol.* **2021**, *19* (8), 484.
(37) Magana, M.; Sereti, C.; Ioannidis, A.; Mitchell, C. A.; Ball, A. R.; Magiorkinis, E.; Chatzipanagiotou, S.; Hamblin, M. R.; Hadjifrangiskou, M.; Tegos, G. P. Options and Limitations in Clinical Investigation of Bacterial Biofilms. *Clin. Microbiol. Rev.* **2018**, *31* (3), No. cmr.00084-16.
(38) Schlafer, S.; Meyer, R. L. Confocal Microscopy Imaging of the Biofilm Matrix. *J. Microbiol. Methods* **2017**, *138*, 50−59.
(39) Neu, T. R.; Lawrence, J. R. Innovative Techniques, Sensors, and Approaches for Imaging Biofilms at Different Scales. *Trends Microbiol.* **2015**, *23* (4), 233−242.
(40) Lagree, K.; Desai, J. V.; Finkel, J. S.; Lanni, F. Microscopy of Fungal Biofilms. *Curr. Opin. Microbiol.* **2018**, *43*, 100−107.
(41) Banerjee, S. Image Processing of Biofilms and Its Applications. In *A Complete Guidebook on Biofilm Study*; Roy, D., Ed.; Elsevier, 2022; pp 287−306, DOI: 10.1016/B978-0-323-88480-8.00012-1.
(42) Hermanowicz, S. W.; Schindler, U.; Wilderer, P. Fractal Structure of Biofilms: New Tools for Investigation of Morphology. *Water Sci. Technol.* **1995**, *32* (8), 99−105.
(43) Neu, T. R.; Lawrence, J. R. One-Photon versus Two-Photon Laser Scanning Microscopy and Digital Image Analysis of Microbial Biofilms. *Methods in Microbiology*; Elsevier B.V., 2004; Vol. *34*, pp 89−136, DOI: 10.1016/S0580-9517(04)34004-3.
(44) Chávez de Paz, L. E. Image Analysis Software Based on Color Segmentation for Characterization of Viability and Physiological Activity of Biofilms. *Appl. Environ. Microbiol.* **2009**, *75* (6), 1734−1739.
(45) Wuertz, S.; Okabe, S.; Hausner, M. Microbial Communities and Their Interactions in Biofilm Systems: An Overview. *Water Sci. Technol.* **2004**, *49* (11−12), 327−336.
(46) Zhang, M.; Zhang, J.; Wang, Y.; Wang, J.; Achimovich, A. M.; Acton, S. T.; Gahlmann, A. Non-Invasive Single-Cell Morphometry in Living Bacterial Biofilms. *Nat. Commun.* **2020**, *11* (1), 6151.
(47) Cinquin, B.; Lopes, F. Structure and Fluorescence Intensity Measurements in Biofilms. In *Computer Optimized Microscopy: Methods and Protocols*; Rebollo, E., Bosch, M., Eds.; Springer New York: New York, NY, 2019; pp 117−133, DOI: 10.1007/978-1-4939-9686-5_7.

https://doi.org/10.1021/acsomega.2c07255
ACS Omega 2023, 8, 20163−20177

(48) Baudin, M.; Cinquin, B.; Sclavi, B.; Pareau, D.; Lopes, F. Understanding the Fundamental Mechanisms of Biofilms Development and Dispersal: BIAM (Biofilm Intensity and Architecture Measurement), a New Tool for Studying Biofilms as a Function of Their Architecture and Fluorescence Intensity. *J. Microbiol. Methods* **2017**, *140*, 47−57.
(49) Bogachev, M. I.; Volkov, V. Y.; Markelov, O. A.; Trizna, E. Y.; Baydamshina, D. R.; Melnikov, V.; Murtazina, R. R.; Zelenikhin, P. V.; Sharafutdinov, I. S.; Kayumov, A. R. Fast and Simple Tool for the Quantification of Biofilm-Embedded Cells Sub-Populations from Fluorescent Microscopic Images. *PLoS One* **2018**, *13* (5), e0193267.
(50) Liu, J.; Dazzo, F. B.; Glagoleva, O.; Yu, B.; Jain, A. K. CMEIAS: A Computer-Aided System for the Image Analysis of Bacterial Morphotypes in Microbial Communities. *Microb. Ecol.* **2001**, *41* (3), 173−194.
(51) Dazzo, F.; Niccum, B. Use of CMEIAS Image Analysis Software to Accurately Compute Attributes of Cell Size, Morphology, Spatial Aggregation and Color Segmentation That Signify in Situ Ecophysiological Adaptations in Microbial Biofilm Communities. *Computation* **2015**, *3* (1), 72−98.
(52) Gross, C. A.; Reddy, C. K.; Dazzo, F. B. CMEIAS Color Segmentation: An Improved Computing Technology to Process Color Images for Quantitative Microbial Ecology Studies at Single-Cell Resolution. *Microb. Ecol.* **2010**, *59* (2), 400−414.
(53) Ji, Z.; Card, K. J.; Dazzo, F. B. CMEIAS JFrad: A Digital Computing Tool to Discriminate the Fractal Geometry of Landscape Architectures and Spatial Patterns of Individual Cells in Microbial Biofilms. *Microb. Ecol.* **2015**, *69* (3), 710−720.
(54) Vorregaard, M.. *Comstat2 - a Modern (3D) Image Analysis Environment for Biofilms*; Technical University of Denmark, 2008.
(55) Yang, X.; Beyenal, H.; Harkin, G.; Lewandowski, Z. Evaluation of Biofilm Image Thresholding Methods. *Water Res.* **2001**, *35* (5), 1149−1158.
(56) Beyenal, H.; Lewandowski, Z.; Harkin, G. Quantifying Biofilm Structure: Facts and Fiction. *Biofouling* **2004**, *20* (1), 1−23.
(57) Kritikos, G.; Banzhaf, M.; Herrera-Dominguez, L.; Koumoutsi, A.; Wartel, M.; Zietek, M.; Typas, A. A Tool Named Iris for Versatile High-Throughput Phenotyping in Microorganisms. *Nat. Microbiol.* **2017**, *2* (5), 17014.
(58) Mueller, L. N.; de Brouwer, J. F.; Almeida, J. S.; Stal, L. J.; Xavier, J. B. Analysis of a Marine Phototrophic Biofilm by Confocal Laser Scanning Microscopy Using the New Image Quantification Software PHLIP. *BMC Ecol.* **2006**, *6*, 10.
(59) Klinger-Strobel, M.; Suesse, H.; Fischer, D.; Pletz, M. W.; Makarewicz, O. A Novel Computerized Cell Count Algorithm for Biofilm Analysis. *PLoS One* **2016**, *11* (5), No. e0154937.
(60) Frühauf, H. M.; Stöckl, M.; Holtmann, D. R-based Method for Quantitative Analysis of Biofilm Thickness by Using Confocal Laser Scanning Microscopy. *Eng. Life Sci.* **2022**, *22* (6), 464−470.
(61) Schneider, C. A.; Rasband, W. S.; Eliceiri, K. W. NIH Image to ImageJ: 25 Years of Image Analysis. *Nat. Methods* **2012**, *9* (7), 671−675.
(62) Abramoff, M.; Magalhães, P.; Ram, S. J. Image Processing with ImageJ. *Biophotonics Int.* **2004**, *11*, 36−42.
(63) Ahrens, J.; Geveci, B.; Law, C. ParaView: An End-User Tool for Large-Data Visualization. In *Visualization Handbook*; Hansen, C. D., Johnson, C. R., Eds.; Butterworth-Heinemann: Burlington, 2005; pp 717−731, DOI: 10.1016/B978-012387582-2/50038-1.
(64) Chiu, C.-L.; Clack, N. Napari: A Python Multi-Dimensional Image Viewer Platform for the Research Community. *Microsc. Microanal.* **2022**, *28* (S1), 1576−1577.
(65) Gingichashvili, S.; Duanis-Assaf, D.; Shemesh, M.; Featherstone, J. D. B.; Feuerstein, O.; Steinberg, D. Bacillus Subtilis Biofilm Development − A Computerized Study of Morphology and Kinetics. *Front. Microbiol.* **2017**, *8* (NOV), 1−9.
(66) Elliott, A. D. Confocal Microscopy: Principles and Modern Practices. *Curr. Protoc. Cytom.* **2020**, *92* (1), No. e68.
(67) Almeida, C.; Azevedo, N. F.; Santos, S.; Keevil, C. W.; Vieira, M. J. Discriminating Multi-Species Populations in Biofilms with Peptide Nucleic Acid Fluorescence In Situ Hybridization (PNA FISH). *PLoS One* **2011**, *6* (3), No. e14786.
(68) Dalton, T.; Dowd, S. E.; Wolcott, R. D.; Sun, Y.; Watters, C.; Griswold, J. A.; Rumbaugh, K. P. An In Vivo Polymicrobial Biofilm Wound Infection Model to Study Interspecies Interactions. *PLoS One* **2011**, *6* (11), No. e27317.
(69) Baird, F. J.; Wadsworth, M. P.; Hill, J. E. Evaluation and Optimization of Multiple Fluorophore Analysis of a Pseudomonas Aeruginosa Biofilm. *J. Microbiol. Methods* **2012**, *90* (3), 192−196.
(70) Gratton, E.; VandeVen, M. J. Laser Sources for Confocal Microscopy. In *Handbook of Biological Confocal Microscopy*; Pawley, J., Ed.; Springer US: Boston, MA, 2006; pp 80−125, DOI: 10.1007/978-0-387-45524-2_5.
(71) Nolte, A.; Pawley, J. B.; Höring, L. Non-Laser Light Sources for Three-Dimensional Microscopy. In *Handbook of Biological Confocal Microscopy*; Pawley, J., Ed.; Springer US: Boston, MA, 2006; pp 126−144, DOI: 10.1007/978-0-387-45524-2_6.
(72) Gonzalez, R. C.; Woods, R. E. *Digital Image Processing*, 4th ed.; Pearson India: Upper Saddle River, N.J., 2018.
(73) Kenneth, S.; Russ, J.; Davidson, M. Basic properties of digital images. Olympus. https://www.olympus-lifescience.com/en/microscope-resource/primer/digitalimaging/digitalimagebasics/ (accessed 2022-07-07).
(74) Lyra, M.; Ploussi, A.; Georgantzoglou, A. MATLAB as a Tool in Nuclear Medicine Image Processing. *MATLAB - A Ubiquitous Tool for the Practical Engineer*; InTech, 2011; DOI: 10.5772/19999.
(75) Niblack, W. *An Introduction to Digital Image Processing*; Strandberg Publishing Company: Copenhagen, 1985.
(76) Ekstrom, M. P. *Digital Image Processing Techniques*; Elsevier Science, 2012.
(77) Confocal Microscopy - Introduction. Olympus. https://www.olympus-lifescience.com/en/microscope-resource/primer/techniques/confocal/confocalintro/ (accessed 2023-04-23).
(78) Shotton, D.; White, N. Confocal Scanning Microscopy: Three-Dimensional Biological Imaging. *Trends Biochem. Sci.* **1989**, *14* (11), 435−439.
(79) Kadam, S.; Madhusoodhanan, V.; Dhekane, R.; Bhide, D.; Ugale, R.; Tikhole, U.; Kaushik, K. S. Milieu Matters: An in Vitro Wound Milieu to Recapitulate Key Features of, and Probe New Insights into, Mixed-Species Bacterial Biofilms. *Biofilm* **2021**, *3* (March), No. 100047.
(80) Tolker-Nielsen, T.; Sternberg, C. Methods for Studying Biofilm Formation: Flow Cells and Confocal Laser Scanning Microscopy. *Methods Mol. Biol.* **2014**, *1149*, 615−629.
(81) Samarian, D. S.; Jakubovics, N. S.; Luo, T. L.; Rickard, A. H. Use of a High-Throughput in Vitro Microfluidic System to Develop Oral Multi-Species Biofilms. *J. Vis. Exp.* **2014**, No. 94, 1−10.
(82) Luo, T. L.; Eisenberg, M. C.; Hayashi, M. A. L.; Gonzalez-Cabezas, C.; Foxman, B.; Marrs, C. F.; Rickard, A. H. A Sensitive Thresholding Method for Confocal Laser Scanning Microscope Image Stacks of Microbial Biofilms. *Sci. Rep.* **2018**, *8* (1), 13013.
(83) Allkja, J.; Bjarnsholt, T.; Coenye, T.; Cos, P.; Fallarero, A.; Harrison, J. J.; Lopes, S. P.; Oliver, A.; Pereira, M. O.; Ramage, G.; Shirtliff, M. E.; Stoodley, P.; Webb, J. S.; Zaat, S. A. J.; Goeres, D. M.; Azevedo, N. F. Minimum Information Guideline for Spectrophotometric and Fluorometric Methods to Assess Biofilm Formation in Microplates. *Biofilm* **2020**, *2*, No. 100010.
(84) Kragh, K. N.; Alhede, M.; Kvich, L.; Bjarnsholt, T. Into the Well—A Close Look at the Complex Structures of a Microtiter Biofilm and the Crystal Violet Assay. *Biofilm* **2019**, *1*, No. 100006.
(85) Allkja, J.; van Charante, F.; Aizawa, J.; Reigada, I.; Guarch-Pérez, C.; Vazquez-Rodriguez, J. A.; Cos, P.; Coenye, T.; Fallarero, A.; Zaat, S. A. J.; Felici, A.; Ferrari, L.; Azevedo, N. F.; Parker, A. E.; Goeres, D. M. Interlaboratory Study for the Evaluation of Three Microtiter Plate-Based Biofilm Quantification Methods. *Sci. Rep.* **2021**, *11* (1), 13779.
(86) Lourenço, A.; Coenye, T.; Goeres, D. M.; Donelli, G.; Azevedo, A. S.; Ceri, H.; Coelho, F. L.; Flemming, H.-C.; Juhna, T.; Lopes, S. P.; Oliveira, R.; Oliver, A.; Shirtliff, M. E.; Sousa, A. M.; Stoodley, P.;

https://doi.org/10.1021/acsomega.2c07255
ACS Omega 2023, 8, 20163−20177

Pereira, M. O.; Azevedo, N. F. Minimum Information about a Biofilm Experiment (MIABiE): Standards for Reporting Experiments and Data on Sessile Microbial Communities Living at Interfaces. *Pathog. Dis.* **2014**, *70* (3), 250−256.
(87) Pettygrove, B. A.; Smith, H. J.; Pallister, K. B.; Voyich, J. M.; Stewart, P. S.; Parker, A. E. Experimental Designs to Study the Aggregation and Colonization of Biofilms by Video Microscopy With Statistical Confidence. *Front. Microbiol.* **2022**, *12*, 785182.
(88) Pawley, J. The 39 Steps: A Cautionary Tale of Quantitative 3-D Fluorescence Microscopy. *Biotechniques* **2000**, *28* (5), 884−887.
(89) Wilson, T.; Masters, B. R. Confocal Microscopy. *Appl. Opt.* **1994**, *33* (4), 565.
(90) Jonkman, J.; Brown, C. M. Any Way You Slice It-A Comparison of Confocal Microscopy Techniques. *J. Biomol. Technol.* **2015**, *26* (2), 54−65.
(91) North, A. J. Seeing Is Believing? A Beginners' Guide to Practical Pitfalls in Image Acquisition. *J. Cell Biol.* **2006**, *172* (1), 9−18.
(92) Murray, J. M. Practical Aspects of Quantitative Confocal Microscopy. *Methods Cell Biol.* **2007**, *81* (06), 467−478.
(93) Thierry, L.; José, A.; Seitz, A. Confocal Microscopy in a Nutshell. Wiley Analytical Science. https://analyticalscience.wiley.com/do/10.1002/imaging.5629/full/, 2016.
(94) Inoué, S. Foundations of Confocal Scanned Imaging in Light Microscopy. In *Handbook of Biological Confocal Microscopy*; Pawley, J., Ed.; Springer US: Boston, MA, 2006; pp 1−19, DOI: 10.1007/978-0-387-45524-2_1.
(95) Rietdorf, J.; Stelzer, E. H. K. Special Optical Elements. In *Handbook of Biological Confocal Microscopy*; Pawley, J., Ed.; Springer US: Boston, MA, 2006; pp 43−58, DOI: 10.1007/978-0-387-45524-2_3.
(96) *Fluorescent and Luminescent Probes for Biological Activity a Practical Guide to Technology for Quantitative Real-Time Analysis*; Mason, W. T., Ed.; Academic Press, 1999.
(97) Tsien, R. Y.; Ernst, L.; Waggoner, A. Fluorophores for Confocal Microscopy: Photophysics and Photochemistry. In *Handbook of Biological Confocal Microscopy*; Pawley, J., Ed.; Springer US: Boston, MA, 2006; pp 338−352, DOI: 10.1007/978-0-387-45524-2_16.
(98) Thermofisher Scientific. Fluorescence Spectraviewer. Thermofisher Scientific. https://www.thermofisher.com/order/fluorescence-spectraviewer?gclid=Cj0KCQiA37KbBhDgARIsAIzce144wDvg0qaEW1bYBboM_Ht_0h7z-_wLaZ0cR7sEt6n8eHYpaj6hwxwaAiP4EALw_wcB&ef_id=Cj0KCQiA37KbBhDgARIsAIzce144wDvg0qaEW1bYBboM_Ht_0h7z-_wLaZ0cR7sEt6n8eHYpaj6hwxwaAiP4 (access date: Nov 21, 2022).
(99) Waters, J. C. Accuracy and Precision in Quantitative Fluorescence Microscopy. *J. Cell Biol.* **2009**, *185* (7), 1135−1148.
(100) Stelzer, E. H. K. The Intermediate Optical System of Laser-Scanning Confocal Microscopes. In *Handbook of Biological Confocal Microscopy*; Pawley, J., Ed.; Springer US: Boston, MA, 2006; pp 207−220, DOI: 10.1007/978-0-387-45524-2_9.
(101) Pawley, J. B. Fundamental Limits in Confocal Microscopy. In *Handbook of Biological Confocal Microscopy*; Pawley, J., Ed.; Springer US: Boston, MA, 2006; pp 20−42, DOI: 10.1007/978-0-387-45524-2_2.
(102) Wilson, T. The Role of the Pinhole in Confocal Imaging System. In *Handbook of Biological Confocal Microscopy*; Pawley, J., Ed.; Springer US: Boston, MA, 1995; Vol. 2, pp 167−182, DOI: 10.1007/978-1-4757-5348-6_11.
(103) Cox, G.; Sheppard, C. J. R. Practical Limits of Resolution in Confocal and Non-Linear Microscopy. *Microsc. Res. Technol.* **2004**, *63* (1), 18−22.
(104) WILSON, T. Resolution and Optical Sectioning in the Confocal Microscope. *J. Microsc.* **2011**, *244* (2), 113−121.
(105) Terasaki, M. Quantification of Fluorescence in Thick Specimens, with an Application to Cyclin B-GFP Expression in Starfish Oocytes. *Biol. Cell* **2006**, *98* (4), 245−252.
(106) Al-Awadhi, F.; Hurn, M.; Jennison, C. Three-Dimensional Bayesian Image Analysis and Confocal Microscopy. *J. Appl. Stat.* **2011**, *38*, 29−46.
(107) Castleman, K. Multiple Color Fluorescence Imaging in Microscopy. In *Confocal and Two-Photon Microscopy - Foundations, Applications, and Advances*; Diaspro, A., Ed.; Wiley, 2002; pp 285−299.
(108) Parker, A. E.; Christen, J. A.; Lorenz, L.; Smith, H. Optimal Surface Estimation and Thresholding of Confocal Microscope Images of Biofilms Using Beer's Law. *J. Microbiol. Methods* **2020**, *174*, No. 105943.
(109) Egner, A.; Hell, S. W. Aberrations in Confocal and Multi-Photon Fluorescence Microscopy Induced by Refractive Index Mismatch. In *Handbook of Biological Confocal Microscopy*; Pawley, J., Ed.; Springer US: Boston, MA, 2006; pp 404−413, DOI: 10.1007/978-0-387-45524-2_20.
(110) Confocal Microscope Objectives. Olympus. https://www.olympus-lifescience.com/en/microscope-resource/primer/techniques/confocal/confocalobjectives/ (accessed 2023-04-23).
(111) White, N. S. Visualization Systems for Multi-Dimensional Microscopy Images. In *Handbook of Biological Confocal Microscopy*; Pawley, J., Ed.; Springer US: Boston, MA, 2006; pp 280−315, DOI: 10.1007/978-0-387-45524-2_14.
(112) Pawley, J. B. Points, Pixels, and Gray Levels: Digitizing Image Data. In *Handbook of Biological Confocal Microscopy*; Pawley, J., Ed.; Springer US: Boston, MA, 2006; pp 59−79, DOI: 10.1007/978-0-387-45524-2_4.
(113) Nyquist Calculator, Scientific Volume Imaging, https://svi.nl/Nyquist-Calculator, 2023.
(114) Rossner, M.; Yamada, K. M. What's in a Picture? The Temptation of Image Manipulation. *J. Cell Biol.* **2004**, *166* (1), 11−15.
(115) Diaspro, A.; Chirico, G.; Usai, C.; Ramoino, P.; Dobrucki, J. Photobleaching. In *Handbook of Biological Confocal Microscopy*; Pawley, J., Ed.; Springer US: Boston, MA, 2006; pp 690−702, DOI: 10.1007/978-0-387-45524-2_39.
(116) Hibbs, A. R.; MacDonald, G.; Garsha, K. Practical Confocal Microscopy. In *Handbook of Biological Confocal Microscopy*; Pawley, J., Ed.; Springer US: Boston, MA, 2006; pp 650−671, DOI: 10.1007/978-0-387-45524-2_36.
(117) *Leica TCS SP8 SMD for FCS, FLIM and FLCS: User Manual*; Leica Microsystems CMS GmbH (access date: Nov 21, 2022).
(118) Kuehn, M.; Hausner, M.; Bungartz, H.; Wagner, M.; Wilderer, P. A.; Wuertz, S. Automated Confocal Laser Scanning Microscopy and Semiautomated Image Processing for Analysis of Biofilms. *Appl. Environ. Microbiol.* **1998**, *64* (11), 4115−4127.
(119) Sekar, R.; Griebe, T.; Flemming, H. Influence of Image Acquisition Parameters on Quantitative Measurements of Biofilms Using Confocal Laser Scanning Microscopy. *Biofouling* **2002**, *18* (1), 47−56.
(120) Zoom Factor/Z Step Size calculation for correct lateral and axial sampling. Cellular Imaging Advanced Light Microscopy, Flow Cytometry and Electron Microscopy Center Amsterdam. https://www.cellularimaging.nl/tutorials/zoom-factor/ (access date: Nov 21, 2022).
(121) Almoughrabie, S.; Ngari, C.; Briandet, R.; Poulet, V.; Dubois-Brissonnet, F. Mosaic-CLSM Assessment of Bacterial Spatial Distribution in Cosmetic Matrices According to Matrix Viscosity and Bacterial Hydrophobicity. *Cosmetics* **2020**, *7* (2), 32.
(122) CHOW, S. K.; HAKOZAKI, H.; PRICE, D. L.; MACLEAN, N. A. B.; DEERINCK, T. J.; BOUWER, J. C.; MARTONE, M. E.; PELTIER, S. T.; ELLISMAN, M. H. Automated Microscopy System for Mosaic Acquisition and Processing. *J. Microsc.* **2006**, *222* (2), 76−84.
(123) Preibisch, S.; Saalfeld, S.; Tomancak, P. Globally Optimal Stitching of Tiled 3D Microscopic Image Acquisitions. *Bioinformatics* **2009**, *25* (11), 1463−1465.
(124) Jane, D. B. Mosaic Images. Leica Microsystem. https://www.leica-microsystems.com/science-lab/mosaic-images/, 2011.

https://doi.org/10.1021/acsomega.2c07255
ACS Omega 2023, 8, 20163−20177

(125) Keevil, C. W. Rapid Detection of Biofilms and Adherent Pathogens Using Scanning Confocal Laser Microscopy and Episcopic Differential Interference Contrast Microscopy. *Water Sci. Technol.* **2003**, *47* (5), 105−116.
(126) Canette, A.; Deschamps, J.; Briandet, R. High Content Screening Confocal Laser Microscopy (HCS-CLM) to Characterize Biofilm 4D Structural Dynamic of Foodborne Pathogens. In *Foodborne Bacterial Pathogens: Methods and Protocols*; Bridier, A., Ed.; Humana: New York, NY, 2019; Vol. *1918*, pp 171−182, DOI: 10.1007/978-1-4939-9000-9_14.
(127) Ivey, S.; Koshoffer, A.; Sneff, G.; Wang, H. Confocal Microscopy Data: A Primer for Curation. Presented at the Specialized Data Curation Workshop at Johns Hopkins University, 2019; pp 1−9.
(128) Zeiss. Overview of Batch Exporting in ZEN Blue. Zeiss (access date: Nov 21, 2022).
(129) Schindelin, J.; Arganda-carreras, I.; Frise, E.; Kaynig, V.; Pietzsch, T.; Preibisch, S.; Rueden, C.; Saalfeld, S.; Schmid, B.; Tinevez, J.; White, D. J.; Hartenstein, V.; Tomancak, P.; Cardona, A. Fiji - an Open Source Platform for Biological Image Analysis. *Nat. Methods* **2012**, *9* (7), 676.
(130) G, M.; Hidalgo, A. Image Processing Methods for Automatic Cell Counting In Vivo or In Situ Using 3D Confocal Microscopy. *Advanced Biomedical Engineering*; InTech, 2011; Vol. *32*, pp 1854−1858, DOI: 10.5772/23147.
(131) Roysam, B.; Lin, G.; Abdul-Karim, M.-A.; Al-Kofahi, O.; Al-Kofahi, K.; Shain, W.; Szarowski, D. H.; Turner, J. N. Automated Three-Dimensional Image Analysis Methods for Confocal Microscopy. In *Handbook of Biological Confocal Microscopy*; Pawley, J., Ed.; Springer US: Boston, MA, 2006; pp 316−337, DOI: 10.1007/978-0-387-45524-2_15.
(132) Beyenal, H.; Donovan, C.; Lewandowski, Z.; Harkin, G. Three-Dimensional Biofilm Structure Quantification. *J. Microbiol. Methods* **2004**, *59* (3), 395−413.
(133) Yerly, J.; Hu, Y.; Jones, S. M.; Martinuzzi, R. J. A Two-Step Procedure for Automatic and Accurate Segmentation of Volumetric CLSM Biofilm Images. *J. Microbiol. Methods* **2007**, *70* (3), 424−433.
(134) Pal, N. R.; Pal, S. K. A Review on Image Segmentation Techniques. *Pattern Recognit.* **1993**, *26* (9), 1277−1294.
(135) Unnikrishnan, R.; Pantofaru, C.; Hebert, M. Toward Objective Evaluation of Image Segmentation Algorithms. *IEEE Trans. Pattern Anal. Mach. Intell.* **2007**, *29* (6), 929−944.
(136) Chaubey, A. K. Comparison of The Local and Global Thresholding Methods in Image Segmentation. *World J. Res. Rev.* **2016**, *2* (1), 1−4.
(137) Beucher, S. The Watershed Transformation Applied to Image Segmentation. *Scanning Microsc.* **1992**, *6* (28), 299−314.
(138) Bannon, D.; Moen, E.; Schwartz, M.; Borba, E.; Kudo, T.; Greenwald, N.; Vijayakumar, V.; Chang, B.; Pao, E.; Osterman, E.; Graf, W.; Van Valen, D. DeepCell Kiosk: Scaling Deep Learning−Enabled Cellular Image Analysis with Kubernetes. *Nat. Methods* **2021**, *18* (1), 43−45.
(139) McQuin, C.; Goodman, A.; Chernyshev, V.; Kamentsky, L.; Cimini, B. A.; Karhohs, K. W.; Doan, M.; Ding, L.; Rafelski, S. M.; Thirstrup, D.; Wiegraebe, W.; Singh, S.; Becker, T.; Caicedo, J. C.; Carpenter, A. E. CellProfiler 3.0: Next-Generation Image Processing for Biology. *PLOS Biol.* **2018**, *16* (7), No. e2005970.
(140) Derlon, N.; Grütter, A.; Brandenberger, F.; Sutter, A.; Kuhlicke, U.; Neu, T. R.; Morgenroth, E. The Composition and Compression of Biofilms Developed on Ultrafiltration Membranes Determine Hydraulic Biofilm Resistance. *Water Res.* **2016**, *102*, 63−72.
(141) Otsu, N. A Threshold Selection Method from Gray-Level Histograms. *IEEE Trans. Syst. Man. Cybern.* **1979**, *9* (1), 62−66.
(142) Ridler, T. W.; Calvard, S. Picture Thresholding Using an Iterative Selection Method. *IEEE Trans. Syst. Man. Cybern.* **1978**, *8* (8), 630−632.
(143) Wilkinson, M. H. F. Optimizing Edge Detectors for Robust Automatic Threshold Selection: Coping with Edge Curvature and Noise. *Graph. Model. Image Process.* **1998**, *60* (5), 385−401.
(144) Xavier, J. B.; Schnell, A.; Wuertz, S.; Palmer, R.; White, D. C.; Almeida, J. S. Objective Threshold Selection Procedure (OTS) for Segmentation of Scanning Laser Confocal Microscope Images. *J. Microbiol. Methods* **2001**, *47* (2), 169−180.
(145) Stolz, J. F. Structure of Microbial Mats and Biofilms. In *Microbial Sediments*; Riding, R. E., Awramik, S. M., Eds.; Springer Berlin Heidelberg: Berlin, Heidelberg, 2000; pp 1−8, DOI: 10.1007/978-3-662-04036-2_1.
(146) Cai, Y.-M. Non-Surface Attached Bacterial Aggregates: A Ubiquitous Third Lifestyle. *Front. Microbiol.* **2020**, *11*, No. 557035.
(147) Niederdorfer, R.; Peter, H.; Battin, T. J. Attached Biofilms and Suspended Aggregates Are Distinct Microbial Lifestyles Emanating from Differing Hydraulics. *Nat. Microbiol.* **2016**, *1* (12), 16178.
(148) Bay, L.; Kragh, K. N.; Eickhardt, S. R.; Poulsen, S. S.; Gjerdrum, L. M. R.; Ghathian, K.; Calum, H.; Ågren, M. S.; Bjarnsholt, T. Bacterial Aggregates Establish at the Edges of Acute Epidermal Wounds. *Adv. wound care* **2018**, *7* (4), 105−113.
(149) Kobayashi, K. Bacillus Subtilis Pellicle Formation Proceeds through Genetically Defined Morphological Changes. *J. Bacteriol.* **2007**, *189* (13), 4920−4931.
(150) Arnaouteli, S.; Bamford, N. C.; Stanley-Wall, N. R.; Kovács, Á. T. Bacillus Subtilis Biofilm Formation and Social Interactions. *Nat. Rev. Microbiol.* **2021**, *19* (9), 600−614.
(151) Bahamondez-Canas, T. F.; Heersema, L. A.; Smyth, H. D. C. Current Status of In Vitro Models and Assays for Susceptibility Testing for Wound Biofilm Infections. *Biomedicines* **2019**, *7* (2), 34.
(152) Brackman, G.; Coenye, T. In Vitro and In Vivo Biofilm Wound Models and Their Application. In *Advances in Microbiology, Infectious Diseases and Public Health*; Donelli, G., Ed.; Springer International Publishing: Cham, 2015; Vol. *897*, pp 15−32, DOI: 10.1007/5584_2015_5002.
(153) Percival, S. L.; McCarty, S. M.; Lipsky, B. Biofilms and Wounds: An Overview of the Evidence. *Adv. wound care* **2015**, *4* (7), 373−381.
(154) Fazli, M.; Bjarnsholt, T.; Kirketerp-Møller, K.; Jørgensen, B.; Andersen, A. S.; Krogfelt, K. A.; Givskov, M.; Tolker-Nielsen, T. Nonrandom Distribution of Pseudomonas Aeruginosa and Staphylococcus Aureus in Chronic Wounds. *J. Clin. Microbiol.* **2009**, *47* (12), 4084−4089.
(155) Kragh, K. N.; Alhede, M.; Jensen, P. Ø.; Moser, C.; Scheike, T.; Jacobsen, C. S.; Seier Poulsen, S.; Eickhardt-Sørensen, S. R.; Trøstrup, H.; Christoffersen, L.; Hougen, H.-P.; Rickelt, L. F.; Kühl, M.; Høiby, N.; Bjarnsholt, T. Polymorphonuclear Leukocytes Restrict Growth of Pseudomonas Aeruginosa in the Lungs of Cystic Fibrosis Patients. *Infect. Immun.* **2014**, *82* (11), 4477−4486.
(156) Saraswathi, P.; Beuerman, R. W. Corneal Biofilms: From Planktonic to Microcolony Formation in an Experimental Keratitis Infection with Pseudomonas Aeruginosa. *Ocul. Surf.* **2015**, *13* (4), 331−345.
(157) Balcázar, J. L.; Subirats, J.; Borrego, C. M. The Role of Biofilms as Environmental Reservoirs of Antibiotic Resistance. *Front. Microbiol.* **2015**, *6* (OCT), 1−9.
(158) Solanki, M. K.; Solanki, A. C.; Kumari, B.; Kashyap, B. K.; Singh, R. K. Plant and Soil-Associated Biofilm-Forming Bacteria: Their Role in Green Agriculture. In *New and Future Developments in Microbial Biotechnology and Bioengineering: Microbial Biofilms*; Yadav, M. K., Singh, B. P., Eds.; Elsevier, 2020; pp 151−164, DOI: 10.1016/B978-0-444-64279-0.00012-8.
(159) Di Pippo, F.; Congestri, R. Culturing Toxic Benthic Blooms: The Fate of Natural Biofilms in a Microcosm System. *Microorganisms* **2017**, *5* (3), 46.
(160) Le Norcy, T.; Faÿ, F.; Obando, C. Z.; Hellio, C.; Réhel, K.; Linossier, I. A New Method for Evaluation of Antifouling Activity of Molecules against Microalgal Biofilms Using Confocal Laser Scanning Microscopy-Microfluidic Flow-Cells. *Int. Biodeterior. Biodegradation* **2019**, *139*, 54−61.
(161) Blanchette-Cain, K.; Hinojosa, C. A.; Akula Suresh Babu, R.; Lizcano, A.; Gonzalez-Juarbe, N.; Munoz-Almagro, C.; Sanchez, C. J.; Bergman, M. A.; Orihuela, C. J. Streptococcus Pneumoniae Biofilm

Formation Is Strain Dependent, Multifactorial, and Associated with Reduced Invasiveness and Immunoreactivity during Colonization. *MBio* **2013**, *4* (5), e00745−13.
(162) Kragh, K. N.; Hutchison, J. B.; Melaugh, G.; Rodesney, C.; Roberts, A. E. L.; Irie, Y.; Jensen, P. Ø.; Diggle, S. P.; Allen, R. J.; Gordon, V.; Bjarnsholt, T. Role of Multicellular Aggregates in Biofilm Formation. *MBio* **2016**, *7* (2), e00237-16.
(163) Xiao, J.; Klein, M. I.; Falsetta, M. L.; Lu, B.; Delahunty, C. M.; Yates, J. R.; Heydorn, A.; Koo, H. The Exopolysaccharide Matrix Modulates the Interaction between 3D Architecture and Virulence of a Mixed-Species Oral Biofilm. *PLoS Pathog.* **2012**, *8* (4), No. e1002623.
(164) Zarabadi, M. P.; Paquet-Mercier, F.; Charette, S. J.; Greener, J. Hydrodynamic Effects on Biofilms at the Bio-Interface Using a Microfluidic Electrochemical Cell: Case Study of Pseudomonas Sp. *Langmuir* **2017**, *33* (8), 2041−2049.
(165) Vazquez, N. M.; Mariani, F.; Torres, P. S.; Moreno, S.; Galván, E. M. Cell Death and Biomass Reduction in Biofilms of Multidrug Resistant Extended Spectrum β-Lactamase-Producing Uropathogenic Escherichia Coli Isolates by 1,8-Cineole. *PLoS One* **2020**, *15* (11), No. e0241978.
(166) Davison, W. M.; Pitts, B.; Stewart, P. S. Spatial and Temporal Patterns of Biocide Action against Staphylococcus Epidermidis Biofilms. *Antimicrob. Agents Chemother.* **2010**, *54* (7), 2920−2927.
(167) Garcia-Betancur, J. C.; Yepes, A.; Schneider, J.; Lopez, D. Single-Cell Analysis of *Bacillus subtilis* Biofilms Using Fluorescence Microscopy and Flow Cytometry. *J. Vis. Exp.* **2012**, No. 60, e3796.
(168) Niggli, S.; Wechsler, T.; Kümmerli, R. Single-Cell Imaging Reveals That Staphylococcus Aureus Is Highly Competitive Against Pseudomonas Aeruginosa on Surfaces. *Front. Cell. Infect. Microbiol.* **2021**, *11*, No. 733991.
(169) Ragi, S.; Rahman, M. H.; Duckworth, J.; Kalimuthu, J.; Chundi, P.; Gadhamshetty, V. Artificial Intelligence-Driven Image Analysis of Bacterial Cells and Biofilms. *IEEE/ACM Trans. Comput. Biol. Bioinforma.* **2021**, 174.

https://doi.org/10.1021/acsomega.2c07255
ACS Omega 2023, 8, 20163−20177